

Asian Journal of  
**Cell Biology**

ISSN 1814-0068



Academic  
Journals Inc.

[www.academicjournals.com](http://www.academicjournals.com)

## **Effect of *Nigella sativa* L. and Thymoquinone on Streptozotocin Induced Cellular Damage in Pancreatic Islets of Rats**

<sup>1</sup>N.E. Abdelmeguid, <sup>2</sup>R. Fakhoury, <sup>3</sup>S.M. Kamal and <sup>2</sup>R.J. AlWafai

<sup>1</sup>Department of Zoology, Faculty of Science, Alexandria University, Moharram Bey, Alexandria 2151, Egypt

<sup>2</sup>Department of Biological and Environmental Sciences, Faculty of Science, Beirut Arab University, Lebanon

<sup>3</sup>Faculty of Medicine, Alexandria University, Alexandria, Egypt

*Corresponding Author: N.E. Abdelmeguid, Department of Zoology, Faculty of Science, Alexandria University, Moharram Bey, Alexandria 2151, Egypt*

### **ABSTRACT**

The aim of the study was to investigate the role of aqueous extract of *Nigella sativa* seed, *Nigella sativa* oil and thymoquinone in ameliorating the cellular damage produced in pancreatic cells by streptozotocin (STZ). Five equal sized groups of male Sprague-Dawley rats were used in this study. The groups included; control, STZ induced diabetic, STZ diabetic-aqueous extract treated (2 mL kg<sup>-1</sup>), STZ diabetic-oil treated (0.2 mL kg<sup>-1</sup>) and STZ diabetic-thymoquinone treated (5 mg kg<sup>-1</sup>) groups. After 30 days of treatment, pancreatic tissues of the different groups were examined by the light and transmission electron microscope. The aqueous extract of *N. sativa* reduced some of the cellular damage caused by STZ on  $\beta$  cells. In contrast, the use of its oil exacerbated the destructive effect of STZ. The use of thymoquinone; the active ingredient of *N. sativa*, ameliorated the toxic effects of STZ on pancreatic  $\beta$  cells. The nuclear alterations observed including segregated nucleoli, marginating aggregates of heterochromatin and decreased heterochromatin indicate DNA damage in STZ-treated rats and are consequently responsible for the development of type 1 diabetes. The present study emphasizes that *N. sativa* extracts are effective in reducing the cellular damage caused by STZ. In addition, findings suggest that the active ingredient thymoquinone is the most effective against STZ diabetes as its administration ameliorated most of the pathological changes. This could be attributed to the antioxidant properties of *N. sativa* and thymoquinone that inhibit the cellular damage caused by STZ in pancreatic cells.

**Key words:** *Nigella sativa*, streptozotocin, thymoquinone, type 1 diabetes, ultrastructure

### **INTRODUCTION**

Diabetes mellitus is rapidly emerging as a global health problem that threatens to reach pandemic levels by 2030 (Hossain *et al.*, 2007). It is a group of metabolic diseases characterized by hyperglycemia resulting from defects in insulin secretion, insulin action, or both (ADA., 2008). It also reported that diabetes is classified into type 1 (insulin dependent) that results from the destruction of pancreatic  $\beta$  cells which produce insulin and type 2 (non-insulin dependent) that results from insulin resistance. There is growing evidence that diabetes is usually accompanied by increased production of free radical and/or impairment and reduction of antioxidant defenses leading to the development and progression of diabetic complications (Brownlee, 2005; Arulselvan and Subramanian, 2007). Several mechanisms seem to be involved in the initiation of this oxidative stress which has been reported in experimental diabetes in animals as well as in type

1 and type 2 diabetic patients: glucose autoxidation, protein glycation. Oxidative stress is involved in the origin of type 1 diabetes especially through the destruction of pancreatic  $\beta$  cells (Houcher *et al.*, 2007). The STZ is the most commonly used diabetogenic agent for experimental animals to produce type 1 diabetes by selectively destroying pancreatic  $\beta$  cells (Szkudelski, 2001). The STZ enters the  $\beta$  cell via a glucose transporter and causes alkylation of DNA.

More than 1000 different plants have been described for traditional treatment of diabetes (Marles and Fransworth, 1994). *Nigella sativa* belongs to the *Ranunculaceae* family (Goreja, 2003). The seeds of *N. sativa* (black seed), have long been used in folk medicine for a wide range of illnesses (Schleicher and Saleh, 1998). Black seeds contain over 100 valuable components and about 30% w/w of a fixed oil and 0.4-0.45% w/w of a volatile oil (El-Tahir *et al.*, 1993a). Analysis of its volatile oil revealed that the main active ingredients are thymoquinone, dithymoquinone. The volatile oil has been shown to contain 18.4-24% thymoquinone and 46% monotropenes (El-Tahir *et al.*, 1993a). The fixed oil is composed mainly of unsaturated fatty acids (Houghton *et al.*, 1995). *Nigella sativa* seeds have been reported to possess antimicrobial (El-Alfy *et al.*, 1975), antibacterial (El-Kamali *et al.*, 1998), antioxidant (Burits and Bucar, 2000; Al-Enazi, 2007), anti-inflammatory (Houghton *et al.*, 1995), antitumoral (Worthen *et al.*, 1998), antihypertensive (El-Tahir *et al.*, 1993b) and hypoglycemic properties (Al-Hader *et al.*, 1993; El-Dakhkhny *et al.*, 2002; Houcher *et al.*, 2007). The aim of this study was to investigate the role of *Nigella sativa* L. seed aqueous extract, oil and its active ingredient thymoquinone in protecting against cellular damage of pancreatic cells in STZ-induced diabetic rats, using light and transmission electron microscope.

## MATERIALS AND METHODS

The present study was carried out during 2009-2010 as part of PhD project at the animal house, Faculty of Pharmacy and Faculty of Science; Beirut Arab University, Beirut, Lebanon.

**Animals and chemicals:** Thirty adult male Sprague Dawley rats (*Rattus norvegicus*), weighing approximately 200 g each and with an average age of 16 weeks were used. A stock of inbreeding rats was obtained by brother sister mating in the animal house of Beirut Arab University, Lebanon, during May 2009. Rats were maintained in 12 h light: dark cycles at constant temperature of  $22\pm 2^\circ\text{C}$ . Rats were kept in plastic cages, 6 rats/cage. All rats were fed daily with standard rat pellets and tap water ad libitum. All animals received human care according to the criteria outlined in the Guide for the Care and Use of Laboratory Animals prepared by the National Academy of Sciences and published by the National Institutes of Health.

Streptozotocin (STZ) antibiotic was purchased from Fluka. Fresh solutions were prepared at a concentration of  $30\text{ mg mL}^{-1}$  buffer by dissolving 0.3 g of STZ in 10 mL of 5 mM citrate buffer pH 4.5 (Ganda *et al.*, 1976). The active ingredient of *N. sativa*, thymoquinone (TQ>99% pure with chemical formula 2-Isopropyl-5-methyl-1, 4-benzoquinone), was purchased from Sigma-Aldrich. Its stock solution was prepared by dissolving 1 g in 10 mL ethanol. Diluted solution of thymoquinone at a concentration of  $3\text{ mg mL}^{-1}$  was prepared by dissolving 300  $\mu\text{L}$  of the stock solution in 10 mL sterile distilled water.

*Nigella sativa* seeds were purchased from a local herb store in Beirut. Its aqueous extract was prepared fresh daily by boiling 2.5 g of seeds in drinking water for 10 min and adjusting the final

volume to 50 mL (to obtain 5% decoction). The solution was then filtered through 4 layers of surgical gauze (Farida *et al.*, 1987). *Nigella sativa* oil was purchased from a local pharmacy in Beirut.

**Experimental design:** The animals were divided into five equal sized groups and treated as follows:

- The control group (GA) was injected with the same volume of citrate buffer as the diabetic groups received
- Diabetes was induced in all groups except group A by a single intraperitoneal (ip) injection of STZ (50 mg kg<sup>-1</sup> body weight, c.f. Kanter *et al.*, 2004), freshly dissolved in citrate buffer pH 4.5. One day after STZ injection, diabetes was confirmed by measuring blood glucose levels in blood samples taken from tail vein. Rats with blood glucose  $\geq 250$  mg dL<sup>-1</sup> were considered diabetic
- The rats in the aqueous extract treated group (GC) were i.p injected with freshly prepared 5% *N. sativa* aqueous extract (2 mL kg<sup>-1</sup>), 6 days/week
- Animals of group GD were i.p. injected 6 days/week by *N. sativa* oil (0.2 mL kg<sup>-1</sup>)
- Rats of the thymoquinone treated group (GE) were i.p. injected with TQ (3 mg mL<sup>-1</sup>) 6days/week at a dose level of 5 mg kg<sup>-1</sup>

It is important to note that animals were not treated with insulin during the experiment (which lasted 30 days). Twenty four hours after the last injection, randomly selected animals from all groups were killed by cervical dislocation. Rats were dissected and small blocks of pancreatic tissues (1 mm<sup>3</sup>) of different groups were removed and dropped quickly into formalin glutaraldehyde fixative (4F<sub>1</sub>G) buffered with 0.1 M phosphate buffer (pH 7.4) and kept at 40°C for around 1 h. After washing twice with buffer (for a period of 4 h), the samples were post-fixed in 1% buffered OsO<sub>4</sub> for 2 h at 4°C. The tissue pieces were washed twice in phosphate buffer for 30 min and then dehydrated in ascending ethanol concentration transferred to propylene oxide and then embedded in 1:1 of Epon: Araldite mixture. Polymerization was done in the oven at 60°C for 24 h. Semithin sections (1 µm) were cut on LKB ultratome with a glass knife and were stained with toluidine blue. Ultrathin sections (50 nm), mounted on copper grids, double stained with uranyl acetate and lead citrate (Reynolds, 1963) and investigated on a JEOL 100CX TEM.

**Statistical analysis:** One way Analysis of Variance (ANOVA) was used to assess significant changes as a result of different treatments. Least Significant Difference (LSD) at 0.05 and 0.01 level of significance was used to test differences among means when analysis of variance indicated significant (p<0.05) result.

## RESULTS

**Control Rats (GA) preparations:** Light preparations of the pancreas of control rats (GA), showed normal architecture. The islets of Langerhans appeared as lightly stained round clusters of cells embedded in the exocrine tissue, surrounded by a thin capsule of reticular connective tissue separating it from adjacent exocrine tissue (Fig. 1a). The islets consisted of polygonal cells with pleomorphic nuclei forming a network separated by blood capillaries (Fig. 1b). Moreover, electron micrographs of islets of Langerhans of this group, revealed the presence of different hormone synthesizing cells that could not be identified with LM.

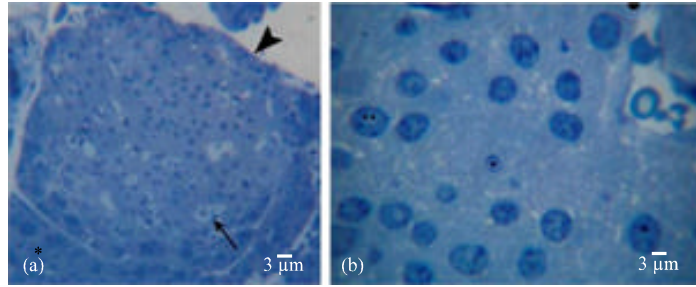


Fig. 1: L.M. Islets of Langerhans of control rats (GA). (a) Illustrating, normal architecture of the pancreas, round islet appearing as a lightly stained cluster of cells (arrow head) compared to the surrounding exocrine pancreatic tissue (asterisk), and blood capillaries (arrow) and surrounded by a thin capsule of reticular connective tissue separating it from the adjacent exocrine pancreatic tissue. (b) Showing, polygonal cells with nuclei of small (asterisk) and large (double asterisk) sizes, prominent nucleoli (Nu), evenly distributed chromatin both centrally and peripherally, and cross section of blood capillary (arrow)

Glucagon or  $\alpha$  producing cell (Fig. 2a, b) were identified by the presence of dense granules with uniform sizes ( $0.21\pm 0.01 \mu\text{m}$  mean diameter) with indistinct limiting membrane that were evenly distributed in the cytoplasm. These cells appeared with various shapes (Fig. 2a, b) and most of them possessed more or less oval nuclei ( $5.700\pm 0.03 \mu\text{m}$  L and  $4.550\pm 0.05 \mu\text{m}$  W) (Fig. 3a). The nucleoli appeared spherical in shape and the chromatin appeared normal in distribution. The membranes of the nuclear envelope appeared indistinct with few nuclear pores (Fig. 2a, b). Concerning mitochondria, few were seen randomly scattered within the cytoplasm. Electron micrographs revealed that most of them showed pale matrices and visible cristae extending to various lengths across the organelle (Fig. 2a, b). Morphometric measurement showed that elongated mitochondria possess  $0.89\pm 0.12 \mu\text{m}$  L and  $0.31\pm 0.02 \mu\text{m}$  W (Fig. 3b) and round mitochondria have an average diameter equal  $0.41\pm 0.01 \mu\text{m}$  (Fig. 3c). In addition, well developed Golgi apparatus (Fig. 2a) and RER in the form of strictly parallel arranged cisterna (Fig. 2b) were observed. Numerous free ribosomes were found to be scattered within cytoplasm (Fig. 2a, b).

The  $\beta$  or insulin producing cells of control rats (GA) were identified by the presence of their characteristic secretory granules which possess a dense core separated by a clear halo from the surrounding limiting membrane. They were polygonal in shape with round basally located nuclei (Fig. 2c, d). Their nuclei possessed  $5.40\pm 0.30 \mu\text{m}$  L and  $4.650\pm 0.05 \mu\text{m}$  W (Fig. 4a). Nuclei of  $\beta$  cells appeared chromatic with an even chromatin distribution (Fig. 2c, d). Membranes of the nuclear envelope appeared distinct (Fig. 2c). Few elongated mitochondria with  $1.08\pm 0.09 \mu\text{m}$  L and  $0.430\pm 0.03 \mu\text{m}$  W (Fig. 4b) were also observed in the cytoplasm (Fig. 2d). In addition, the cytoplasm contained small rounded mitochondria (Fig. 2c) with a dense matrix and tubular cristae. These mitochondria have an average diameter of  $0.48\pm 0.02 \mu\text{m}$  (Fig. 4c). Moreover, a well developed network of Golgi apparatus was observed. Cross sections of rER, free ribosomes, polysomes and numerous rounded secretory granules were also noted in the cytoplasm (Fig. 2d). The ultrastructural observation revealed that these granules were of different sizes and possessed centric or acentric dense cores (Fig. 2c). Also, based on morphometric measurements, statistical analysis revealed that the large granules possessed a mean diameter of  $0.67\pm 0.02 \mu\text{m}$  (Fig. 4d) while small granules possessed a mean diameter of  $0.34\pm 0.02 \mu\text{m}$  (Fig. 4e).

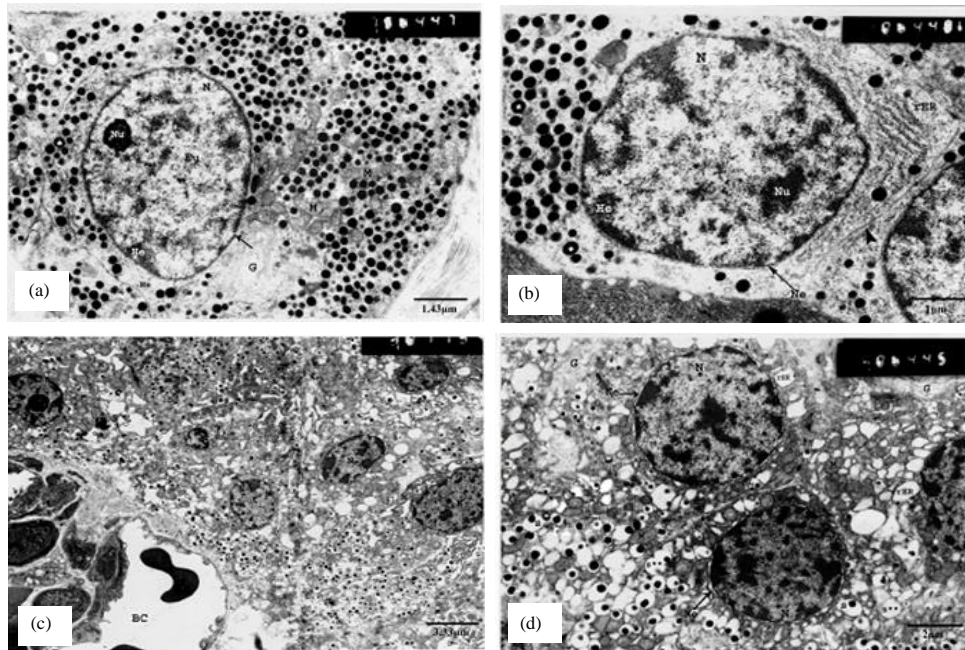


Fig. 2: E.M. Islets of Langerhans of control rats (G A). (a) Showing; part of  $\alpha$ -cell with oval nucleus (N), obvious nucleolus (Nu), finely granular less dense euchromatin (Eu), dense heterochromatin (He), indistinct nuclear envelope (Ne) with few nuclear pores (arrow), mitochondria (M), area of Golgi apparatus (G), and the round shape strongly electron dense characteristic  $\alpha$  secretory granules (asterisk). (b) Illustrating; large nucleus of  $\alpha$  cell with a prominent nucleolus (Nu), evenly distributed heterochromatin (He), a distinct nuclear envelope (Ne), rER cisterna, the characteristic  $\alpha$  secretory granules (asterisk), and the regular cell membrane (arrow head). (c) Illustrating; polygonal  $\beta$  cells with indistinct intercellular spaces scattered around a blood capillary (BC). Note the basally located oval nuclei (N), visible nucleoli (Nu), evenly distributed chromatin, and distinct nuclear envelope (Ne), numerous mitochondria (arrow head), and the characteristic  $\beta$  secretory granules (s) occupying the apical portion of the  $\beta$  cells. (d) Demonstrating; two polygonal  $\beta$  cells, with large sized round nuclei (N) and even distribution of heterochromatin (He), prominent nucleolus (Nu), distinct nuclear envelope (Ne), mitochondria (M) with dark matrices, well developed network of Golgi apparatus (G), rER cisterna (rER), the characteristic  $\beta$  secretory granules (s) of different sizes, secretory granules (s\*) of less dense cores, and very few empty granules (s\*\*)

**Diabetic Rats (GB) preparations:** In contrast to control (GA), semithin sections of pancreas of diabetic rats (GB) revealed that the islets were relatively small, atrophied and clearly showed a reduction in the number of polygonal islet cells (Fig. 5a). At higher magnification, round-ovoid nucleoli of various sizes were observed. Centric and terminalized nucleoli were noted in most of the nuclei (Fig. 5b, c). The distribution of chromatin was abnormal in nuclei of many cells where some areas of the nucleoplasm appear pale. The heterochromatin was noted as clumps scattered in the nucleoplasm or as a fine distinct band restricted to the nuclear envelope. Vacuolation of the

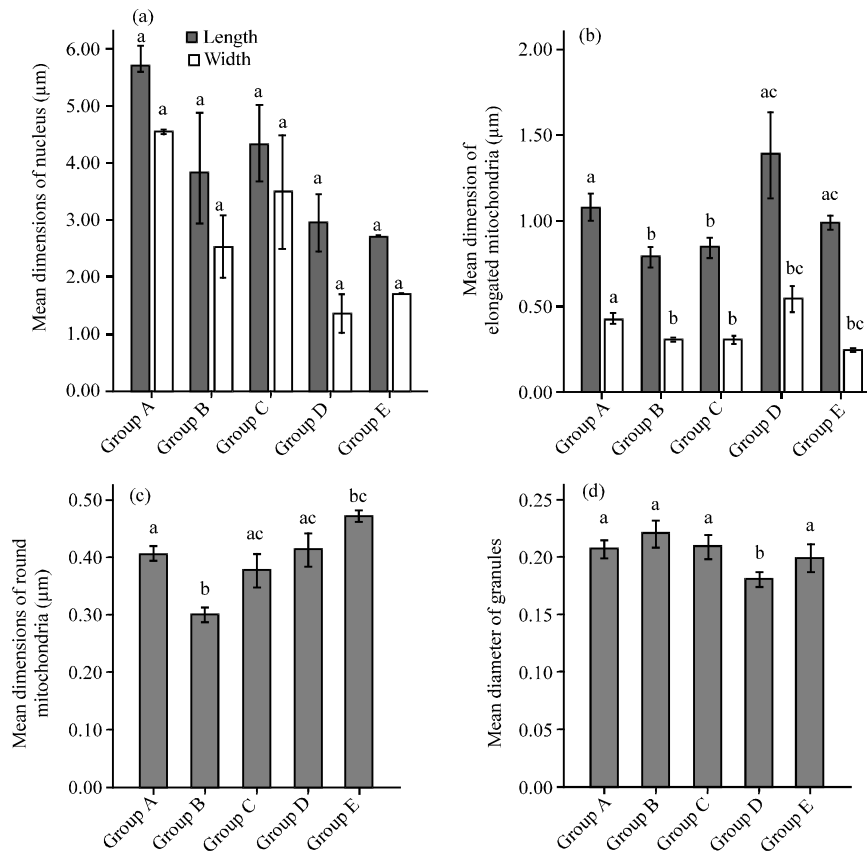


Fig. 3: Morphometric measurements of ultrastructure criteria of  $\alpha$  cells of islets of Langerhans in the different groups. (a) Illustrating changes in the Mean $\pm$ SE nuclear dimensions among the various groups. (b) Demonstrating Mean $\pm$ SE dimensions of elongated mitochondria among various groups. (c) Showing changes in the Mean $\pm$ SE diameter of round mitochondria among various groups. (d) Illustrating changes in the Mean $\pm$ SE diameter of  $\alpha$  secretory granules among various groups. Bars with different superscripts are significantly different ( $p < 0.05$ )

nucleoplasm was noted in some nuclei (Fig. 5c). However, some cells displayed normal chromatin distribution (Fig. 5b, c). Extensive fibrosis was noted in the connective tissue area surrounding blood vessels (Fig. 5d). Insulitis (inflammation of the pancreas) was noted in several islets (Fig. 5b). The cytoplasm appeared homogenous and lightly stained in most cells. However, vacuolation was noted in certain areas of cytoplasm of some cells (Fig. 5c). Also, the most important finding was degranulation in most cells with only few secretory granules observed in certain cells (Fig. 5c). Blood capillaries lined with endothelium and congested with blood were noted in islets (Fig. 5b).

$\alpha$ -cells of islets of diabetic rats (GB) appeared with variously shaped with oval or round nuclei, prominent nucleoli and even distribution of both euchromatin and heterochromatin (Fig. 6a). The nuclei showed insignificant decrease ( $p > 0.05$ ) in dimensions compared to GA. The membranes of the nuclear envelope appeared indistinct. An increased number of nuclear pores were noted when compared to the control (Fig. 6a). The mitochondria were few in number round and elongated and displayed dark matrices (Fig. 6a, b). Statistical analysis revealed significant decrease in the mean diameter of rounded mitochondria and mean width of elongated mitochondria compared to the

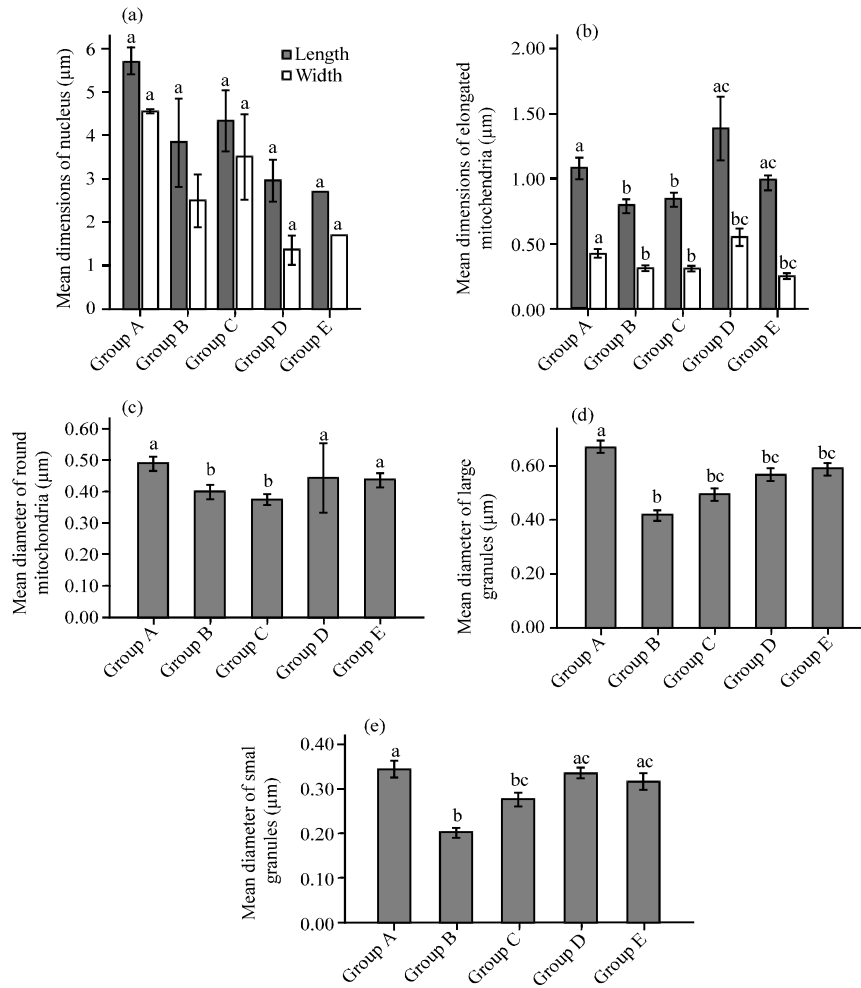


Fig. 4: Morphometric measurements of ultrastructure criteria of  $\beta$  cells of islets of Langerhans in the different groups. (a) Illustrating changes in the Mean $\pm$ SE nuclear dimensions among the various groups. (b) Demonstrating changes in the Mean $\pm$ SE dimensions of elongated mitochondria among various groups. (c) Showing changes in the Mean $\pm$ SE diameter of round mitochondria among the various groups. (d) Illustrating changes in the Mean $\pm$ SE diameter of large  $\beta$  secretory granules among various groups. (e) Demonstrating changes in the Mean $\pm$ SE diameter of small  $\beta$  secretory granules among various groups. Bars with different superscripts are significantly different ( $p < 0.05$ )

control group (Fig. 3b, c). Some cells displayed elongated mitochondria with signs of fragmentation (Fig. 6b). Cisterna of rER and numerous free ribosomes were noted in the cytoplasm (Fig. 6a, b). Moreover, the cytoplasm of these cells contained characteristic dense secretory granules (Fig. 6a, b). These granules possessed  $0.22 \pm 0.01 \mu\text{m}$  mean diameter, demonstrating the highest mean among all experimental groups. However, statistical analysis displayed insignificant increase when compared to GA (Fig. 3d). The cytoplasm appeared disrupted and vacuolated in some cells (Fig. 6b).

On the other hand,  $\beta$  cells of diabetic rat appeared polygonal in shape with oval nuclei (Fig. 7a). Insignificant changes in nuclear dimensions compared to GA (Fig. 4a) were detected. It was noticed



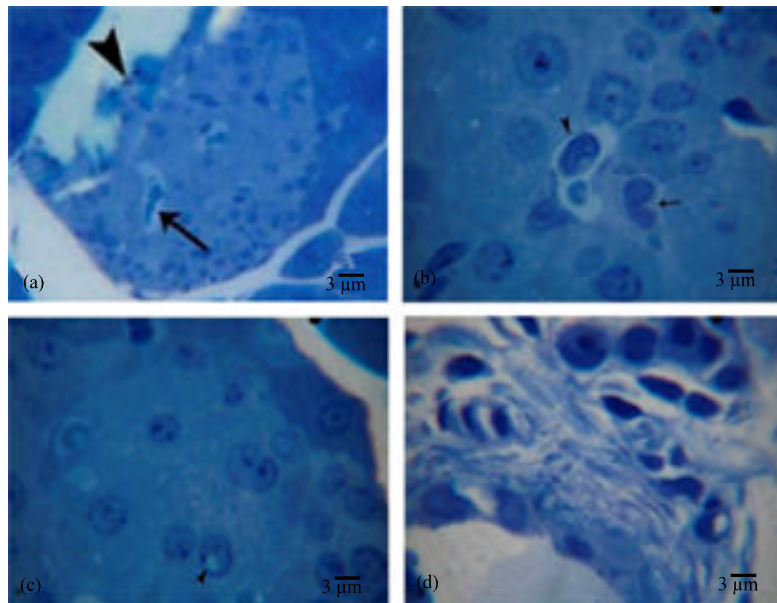


Fig. 5: L.M. Islets of Langerhans of Diabetic rats (GB). (a) Demonstrating a relatively small and atrophic islet (arrow head) with a reduced number of polygonal cells, and cross sections of blood capillaries (arrow) in the islet with erythrocytes and monocytes in their lumen. (b) Showing polygonal cells of islets of Langerhans with pleomorphic round-ovoid nuclei, centric nucleoli (Nu) in some nuclei, and abnormal distribution of chromatin, cross section of blood capillary (arrow) lined with a monocyte in the lumen, and macrophage (arrow head) infiltrating the islet tissue. (c) Showing the cells of islets of Langerhans with round to oval nuclei of various sizes, centric and terminalized nuclei, vacuolation (arrow head) of the nucleoplasm in some nuclei (arrow head), heterochromatin appearing as fine distinct coarse granules of different sizes restricted to the nuclear envelope, lightly stained cytoplasm, and few secretory granules in certain areas appearing as darkly stained spherical structure. (d) Showing extensive fibrosis in the connective tissues area surrounding the blood vessel

that some nuclei displayed normal chromatin distribution, while many others possessed marginating heterochromatin and few nuclei displayed decreased heterochromatin (Fig. 7a-c). Moreover, some cells showed slightly irregular outline nuclei and increased numbers of dilated nuclear pores compared to GA (Fig. 7d). One of the most important findings among this group was the presence of inclusions in some nuclei (Fig. 7c). The nucleoli appeared segregated in some cells (Fig. 7a). The mitochondria assumed both round and elongated shapes with dark matrices and visible cristae. Significant decrease in dimension of mitochondria (Fig. 4b, c) compared to GA was observed. An increased number of small elongated mitochondria were noted in some cells as compared to GA with most of them displaying signs of fragmentation (Fig. 7c). The Golgi and rER cisterna appeared dilated compared to normal (Fig. 7b, d). In addition, free ribosomes were dispersed in the cytoplasm. However, autophagosomes in some cells (Fig. 7b) were observed and the cytoplasm appeared vacuolated in some cells (Fig. 7d) and contained numerous characteristic  $\beta$  secretory granules of two different sizes (Fig. 7b-d). Statistical analysis showed that both types demonstrated significant decrease in diameter compared to the corresponding granules in the

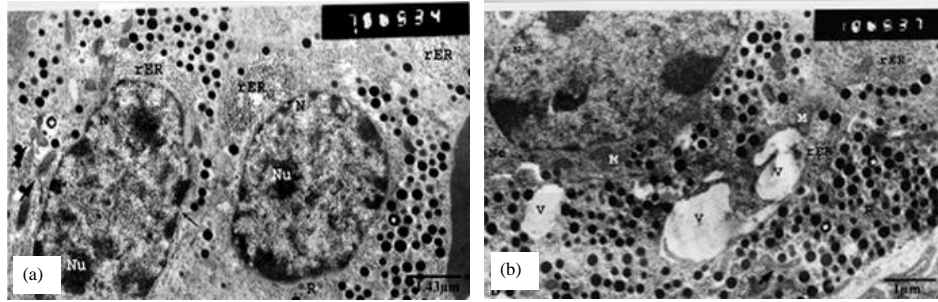


Fig. 6: E.M. Islets of Langerhans of diabetic rats (GB). (a) Demonstrating; the difference in size and shape of  $\alpha$  cell nuclei (N), the prominent nucleoli (Nu), the evenly distributed chromatin, indistinct nuclear envelope (Ne) displaying a number of nuclear pores (arrow), small sized round and elongated mitochondria with black arrow pointing at elongated mitochondria exhibiting signs of fragmentation, the rER cisterna, free ribosomes (R), polysomes as well as the characteristic  $\alpha$  secretory granules (asterisk). (b) Illustrating; part of  $\alpha$  cell nucleus (N), with normal chromatin distribution and indistinct nuclear envelope (Ne), small sized round and elongated mitochondria (M), arrows pointing at elongated mitochondria displaying signs of fragmentation, cisterna of rER, ribosomes (R), as well as the characteristic  $\alpha$  secretory granules (asterisk). Note also very large vacuoles (V) in the disrupted cytoplasm

control group (GA) (Fig. 4d, e). Some cells demonstrated the presence of numerous secretory granules with less dense cores compared to control group (Fig. 7a). In addition, an increased number of empty granules were noted in  $\beta$  cells of these diabetic rats compared to GA (Fig. 7d).

***N. sativa* aqueous extract (GC) treated diabetic rats preparations:** In the diabetic group treated with *N. sativa* aqueous extract (GC), lightly stained small sized round islets (Fig. 8a) with reduced number of polygonal islet cells compared to the control were observed. Nuclei appeared round to ovoid in shape and of various sizes and with terminalized nucleoli in most of them (Fig. 8b). The chromatin appeared reduced in some nuclei displaying pale areas in nucleoplasm (Fig. 8b). However, most nuclei showed normal chromatin distribution. The cytoplasm appeared homogenous with darkly stained spherical secretory granules in certain areas (Fig. 8b).

Electron micrographs showed  $\alpha$  cell of various shapes (Fig. 9a, b). Some cells demonstrated the presence of normal round nuclei; others showed slightly irregular nuclei (Fig. 9a) and some possessed small sized nuclei (Fig. 9b). It is of considerable interest to indicate that the nucleoli appeared terminalized in most nuclei (Fig. 9b). Normal chromatin distribution was noted in the nuclei (Fig. 9b). The membranes of the nuclear envelope appeared distinct in some cells with extensive dilation in the perinuclear spaces (Fig. 9b). Some cells showed nuclear blebbing at certain sites (Fig. 9b). Statistical analysis based on morphometric measurements showed that the dimensions of nuclei displayed insignificant change in comparison to the control group (GA) (Fig. 3a). Round and elongated mitochondria with dark matrices were observed in the cytoplasm of  $\alpha$  cells (Fig. 9a). The number and distribution of the mitochondria did not differ greatly from those of the control group (GA). However, most of the elongated mitochondria noted displayed signs of fragmentation (Fig. 9a). Significant increase in diameter of round mitochondria compared to the

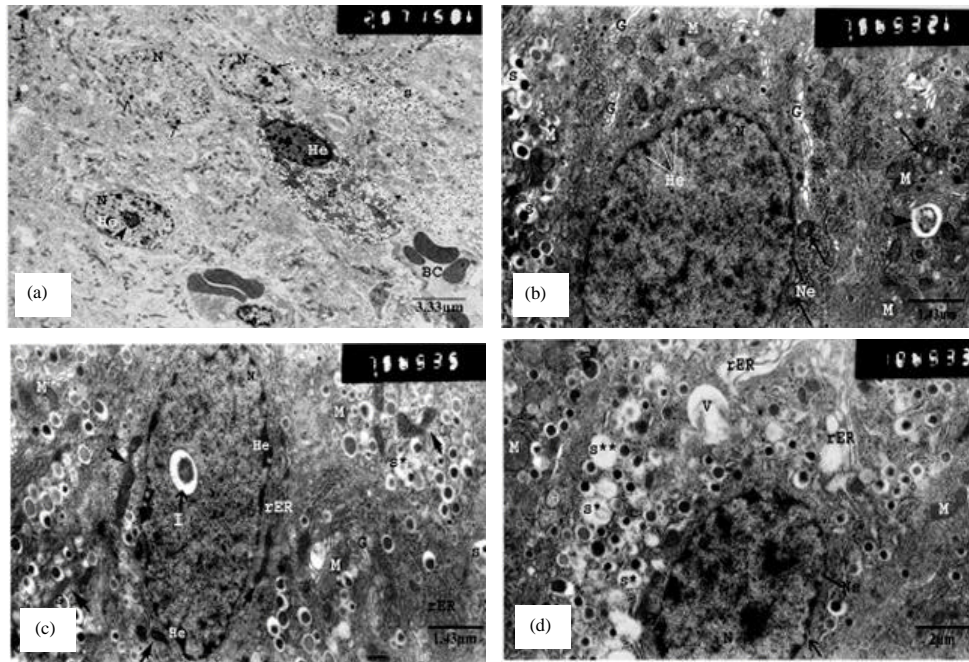


Fig. 7: E.M. Islets of Langerhans of diabetic rats (GB). (a) Illustrating, polygonal  $\beta$  cells with basally located oval nuclei (N), central segregated nucleolus (arrow head), evenly distributed chromatin in some nuclei, decreased heterochromatin (arrow) in the form of clumps marginating the indistinct nuclear envelope (Ne) in others, indistinct intercellular spaces, small sized, the characteristic secretory granules with dense cores (s) and blood capillaries (BC). (b) illustrating; oval shaped nuclei (N), with slightly irregular nuclear envelope (Ne), decreased heterochromatin (He), mitochondria (M), arrows pointing at vacuolated mitochondria, dilated Golgi cisternea (G), autophagosomes in the cytoplasm (arrow head), the characteristic  $\beta$  secretory granules (s),  $\beta$  secretory granules displaying less dense cores (s\*). (c) Demonstrating; oval shaped nucleus (N) housing an inclusion (I) in the nucleoplasm, decreased heterochromatin (He), indistinct nuclear envelope (Ne), round and elongated electron dense mitochondria (M), arrows pointing at the elongated mitochondria displaying signs of fragmentation, the Golgi apparatus (G), the distended rER, and  $\beta$  secretory granules with less dense cores (s\*). (d) Showing large oval shaped nucleus (N) of  $\beta$  cells with prominent nucleolus (Nu), heterochromatin (He) clumps, indistinct nuclear envelope (Ne), round and elongated mitochondria (M), Golgi apparatus (G), dilated rER with membrane bound ribosomes, characteristic  $\beta$  secretory granules of less dense cores (s\*), and empty  $\beta$  secretory granules (s\*\*)

diabetic group (GB) (Fig. 3c) was noticed. The mean width of the elongated mitochondria decreased significantly ( $p < 0.05$ ) compared to control group (GA) while the mean length showed insignificant change (Fig. 3b). Golgi apparatus and few cisternea of rER with membrane bound ribosomes were also noted in the cytoplasm, mainly sequestered in the region of the nucleus (Fig. 9a, b). The cytoplasm of  $\alpha$  cells contained spherical dense secretory granules with a mean diameter equal to  $0.21 \pm 0.01$  (Fig. 3d).

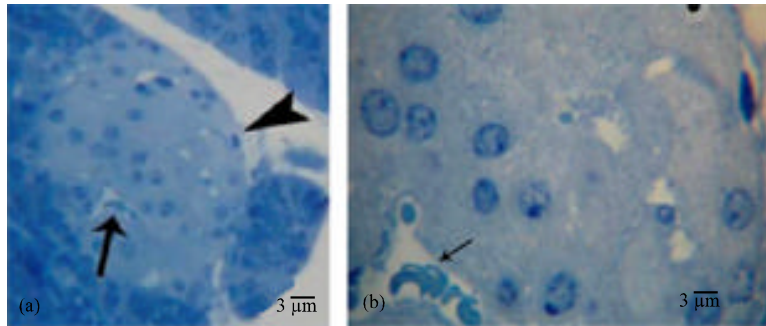


Fig. 8: L.M. Islets of Langerhans of aqueous extract of *Nigella sativa* treated rats (GC). (a) Showing small sized lightly stained round islet (arrow head) with a decreased number of polygonal cells, and cross sections of blood capillaries (arrow) with erythrocytes noted in their lumen. (b) Illustrating cells of islets of Langerhans of the pancreas with pleomorphic nuclei, terminalized nucleoli, pale areas of the nucleoplasm in some nuclei, homogenous and lightly stained cytoplasm, secretory granules in certain areas appearing as darkly stained spherical structure, and a cross section of a blood capillary (arrow)

The  $\beta$  cells of the aqueous extract-treated group (GC) were characterized by a polygonal shape and pleomorphic nuclei. Some cells displayed spherical nuclei (Fig. 9c), others showed irregular shaped nuclei (Fig. 9d) and small sized nuclei were noted in some cells. The nucleoli appeared segregated in most nuclei (Fig. 9c). The heterochromatin showed normal distribution. The nuclear envelope showed distinct membranes and dilated perinuclear space. It is of interest to note that nuclear blebbing was observed at certain sites of the nuclear envelope (Fig. 9c, d). Small sized round and elongated mitochondria with dark matrices were observed scattered in the cytoplasm of  $\beta$  cells of this group (Fig. 9c, d). The number and distribution of mitochondria was similar to that of control (GA). However, some of mitochondria appeared vacuolated (Fig. 9d). Statistical analysis showed that both diameter of round mitochondria and dimensions of elongated mitochondria were significantly decreased ( $p < 0.05$ ) compared to GA (Fig. 4b, c). Dilated Golgi, rER cisterna and free numerous ribosomes were noted dispersed in the cytoplasm (Fig. 9c, d). The cytoplasm of the  $\beta$  cells was filled with  $\beta$  secretory granules of two different sizes (Fig. 9d). Most of them contained a dense core while few displayed less dense cores and very few appeared empty. Statistical analysis showed a significant decrease ( $p < 0.05$ ) in the mean diameter of both small and large secretory granules compared to the control group (GA). Statistical analysis also indicated a significant increase ( $p < 0.05$ ) in diameter of both granules compared to diabetic group (GB) (Fig. 4d, e).

***N. sativa* oil (GD) treated diabetic rats preparations:** Semithin sections of animals treated with oil of *N. sativa* (GD) showed that the islets appeared relatively small and irregularly shaped compared to the control (GA). However, an increase in number of the polygonal islet cells compared to diabetic group (GB) (Fig. 10a) was noticed. Nuclei were pleomorphic in shape with terminalized nuclei in most of them. The nuclei demonstrated normal chromatin distribution (Fig. 10b). However, some nuclei appeared euchromatic (Fig. 10b). The cytoplasm appeared homogenous and lightly stained in some areas with the secretory granules noted. In other areas the cytoplasm appeared disrupted showing small vacuoles and wide intercellular spaces (Fig. 10b). Cross sections of blood capillaries lined with endothelium were noted (Fig. 10b).



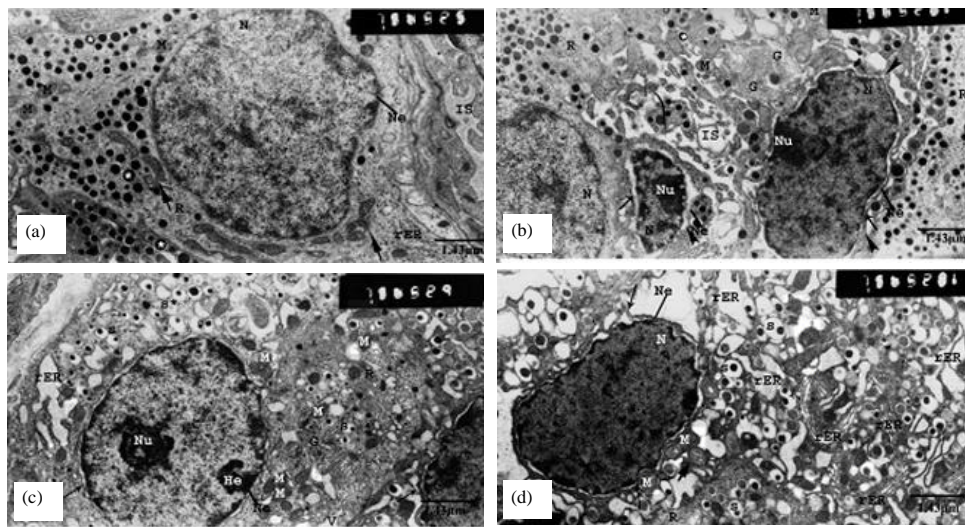


Fig. 9: E.M. Islets of Langerhans of rats treated with aqueous extract of *N. sativa* (GC). (a) Demonstrating; large more or less round  $\alpha$  cell nucleus (N), with slightly irregular nuclear envelope (Ne), indistinct membranes of nuclear envelope (Ne), mitochondria (M), arrows pointing at fragmented mitochondria, rER cisterna,  $\alpha$ -secretory granules (asterisk), and the dilated intracellular space (IS). (b) Illustrating; two  $\alpha$  cells with different sizes and pleomorphic nuclei (N). Note one  $\alpha$  cell with small sized nucleus (N), marginated nucleolus (Nu), normal distribution of heterochromatin, and distinct membranes of the nuclear envelope (Ne) with extensive dilation of the perinuclear space (arrow). Note also  $\alpha$  cell with an irregular outline nucleus (N), with a terminalized nucleolus (Nu), distinct nuclear envelope (Ne), dilated perinuclear space (arrow), and nuclear blebbing at certain sites (arrow head). Notice dense  $\alpha$  secretory granules (asterisk), wide intercellular spaces (IS) between the cells, and disruption of the cytoplasm with the presence of vacuoles. (c) Illustrating;  $\beta$ -cell with a large spherical nucleus (N), segregated nucleolus (Nu), normal chromatin distribution, distinct nuclear envelope (Ne), nuclear blebbing (arrow), and slight dilation of the perinuclear space. Note the small sized round mitochondria (M), diminished Golgi cisterna (G), dilated rER cisterna, small sized characteristic  $\beta$  secretory granules (s), granules with less dense cores (s\*), and cytoplasmic vacuolization (V). (d) Demonstrating;  $\beta$ -cell with an irregular outline nucleus (N), distinct nuclear envelope (Ne), dilated perinuclear space, nuclear blebbing (arrow), mitochondria (M) with black arrow pointing at vacuolated mitochondria, dilated Golgi cisterna (G), dilated rER cisterna, free ribosomes (R), and  $\beta$  secretory granules (s)

Examination of the electron micrographs showed that  $\alpha$  cell displayed some abnormalities. The cells appeared polygonal in shape and possessed oval nuclei with various sizes and dispersed chromatin (Fig. 11a). Some euchromatic nuclei were noted. Membranes of the nuclear envelope appeared distinct in some cells while dilation in the perinuclear space was noted in other cells (Fig. 11a). Very few round and elongated mitochondria were observed in the cytoplasm of the  $\alpha$  cells (Fig. 11a). A significant increase ( $p < 0.05$ ) in the mean diameter of the round mitochondria

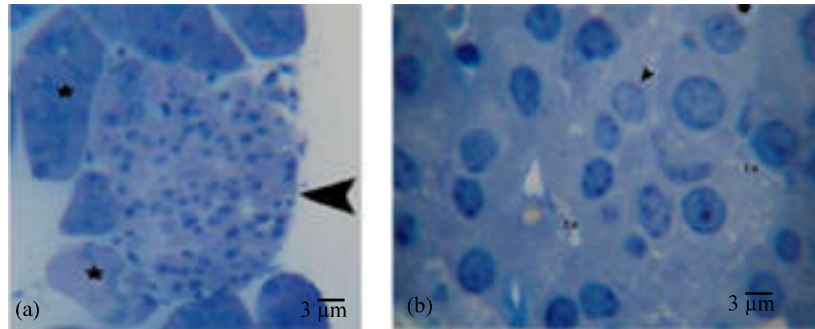


Fig. 10: L.M. Islets of Langerhans of oil of *Nigella sativa* treated rats (GD). (a) Showing relatively small and irregularly shaped islet (arrow head), containing polygonal cells with variously sized nuclei arranged in cords and thin capsule of connective tissue surrounding the islet and separating it from the adjacent exocrine pancreatic tissue (asterisk). (b) Illustrating the polygonal islet cells with nuclei of various sizes, terminalized and centric (asterisk) nucleoli. Note the euchromatic nuclei (arrow head), the disrupted cytoplasm showing small vacuoles, wide intercellular spaces (IS), and secretory granules appearing as darkly stained spherical structure

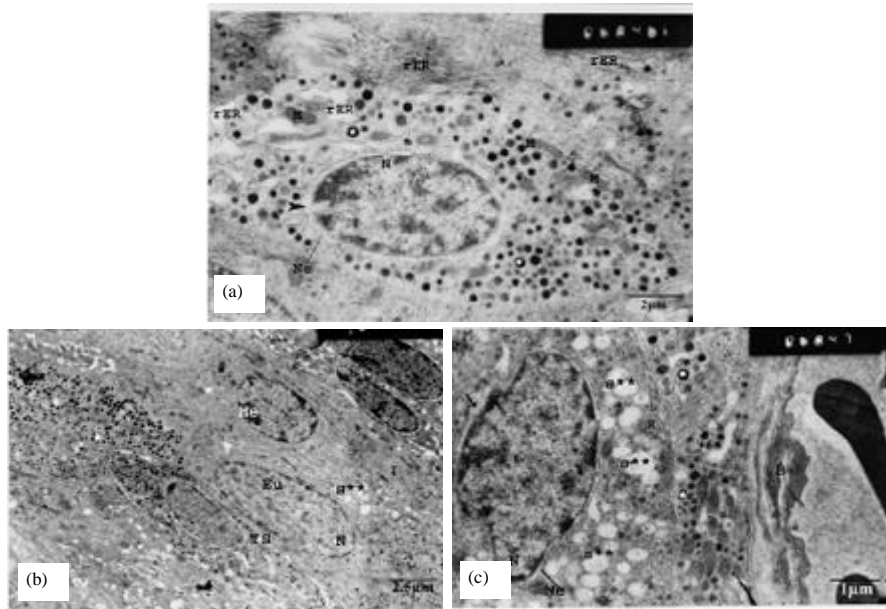


Fig. 11: E.M. Islets of Langerhans of rats treated with oil of *Nigella sativa* (G D). (a) Showing; -cell with an oval nucleus (N), normal distribution of chromatin, distinct nuclear envelope (Ne), dilated perinuclear space (arrow head), the elongated mitochondria (M), dilated rER, and the characteristic dense secretory granules (asterisk). (b) Showing; oval shaped and cells with basally located oval nuclei. Notice the heterochromatic nuclei in cells, empty characteristic secretory granules (s\*\*), distinct intercellular spaces, and vacuolization of the cytoplasm. (c) Illustrating; parts of and -cells in contact with each others. Note the slightly irregular outline nucleus (N) of the cell, the normally distributed chromatin, distinct membranes of the nuclear envelope (Ne), slight dilation of perinuclear space (arrow), the empty characteristic secretory granules (s\*), the intercellular space and the basal lamina (B)

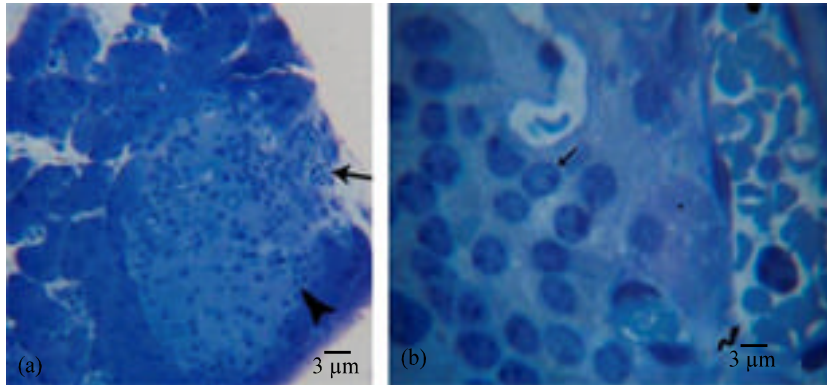


Fig. 12: L.M. Islets of langerhans of Thymoquinone treated rats (GE). (a) Showing, elongated islet (arrow head) consisting of polygonal cells with variously shaped nuclei, arrow pointing at the cross section of blood capillaries congested with erythrocytes. (b) Demonstrating highly disorganized polygonal cells of islets of Langerhans with pleomorphic nuclei of various sizes, terminalized nucleoli in some cells (arrow), disrupted cytoplasm in certain areas displaying small vacuoles, infiltration of the islet by the exocrine acinar (asterisk), and curved arrow pointing at a capillary appearing congested with erythrocytes and neutrophils

compared to the diabetic group (GB) was detected (Fig. 3c) while elongated mitochondria displayed a significant decrease ( $p < 0.05$ ) in dimensions compared to the control group (Fig. 3b). The rER appeared as dilated sections lined with ribosomes (Fig. 11a). Numerous electron dense secretory granules were noted scattered within the cytoplasm. Statistical analysis revealed that secretory granules displayed significant decrease ( $p < 0.05$ ) in the mean diameter of secretory granules compared to the control group (GA) (Fig. 3d). The presence of small cytoplasmic vacuoles indicated disruption of the cytoplasm.

$\beta$  cells of this group showed that cells were polygonal in shape and with pleomorphic nuclei but displayed cellular damage (Fig. 11b). Also, slightly irregular outline nuclei with even chromatin distribution were noted (Fig. 11c). Membranes of the nuclear envelope appeared distinct with slight dilation in perinuclear space (Fig. 11b). A significant decrease ( $p < 0.05$ ) in mean width of nuclei compared to the control (GA) was noticed (Fig. 4a). Very few round and elongated mitochondria were observed in  $\beta$  cells after oil treatment compared to control (GA). Statistical analysis showed significant increase ( $p < 0.05$ ) in dimensions of elongated mitochondria compared to diabetic group (GB). In addition, the mean width of elongated mitochondria showed a significant increase ( $p < 0.05$ ) compared to control (GA) (Fig. 4b). Free ribosomes were noted in the cytoplasm of these cells (Fig. 11c). It is worth mentioning that most of secretory vesicles noted in the cytoplasm were either empty or possessed less dense cores (Fig. 11c). However, few granules displayed characteristic dense cores. Significant decrease ( $p < 0.05$ ) in diameter of large secretory granules compared to control (GA) and a significant increase ( $p < 0.05$ ) compared to diabetic group (GB) were noted (Fig. 4d). On the other hand, the diameter of small secretory granules showed significant increase ( $p < 0.05$ ) compared to induced diabetic group (GB) (Fig. 4e). The cytoplasm appeared disrupted and vacuolated (Fig. 11b).



Fig. 13: E.M. Islets of Langerhans of rats treated with thymoquinone (Group E). Illustrating;  $\alpha$  cell with a small sized nucleus, distinct nuclear envelope (Ne), dilated perinuclear space, round mitochondria (M) with pale matrices, and dilated cross sections of rER cisterna. Note also, part of the cytoplasm of  $\beta$  cells with round and elongated mitochondria (M), Golgi (G), rER and small sized  $\beta$ -secretory granule

**Thymoquinone (GE) treated diabetic rats preparations:** In the diabetic rats treated with thymoquinone (GE), light micrographs of pancreas showed lightly stained elongated islets of similar size to that detected in control (GA). An increase in number of polygonal islet cells was noted compared to diabetic group (GB) (Fig. 12a). Further examination showed round-ovoid nuclei with centric or terminalized nucleoli (Fig. 12b). Normal distribution of chromatin was noted in most nuclei (Fig. 12b). Vacuolation was noted in the nucleoplasm of some nuclei. Disruption of the cytoplasm was noted in certain areas showing small vacuoles (Fig. 12b). In other areas the cytoplasm appeared homogenous and the secretory granules were noted. Infiltration of the islet by the exocrine acinar cells was noted in few islets. Inflammation was noted in certain islets with congested blood capillaries surrounding the islet (Fig. 12b).

Examination of electron micrographs showed that  $\alpha$  cells were variously shaped and demonstrated the presence of small sized heterochromatic nuclei. Membranes of the nuclear envelope (Ne) appeared distinct and dilation in the perinuclear space was also observed (Fig. 13). Round and elongated mitochondria with pale matrices and cristea were noted in the cytoplasm (Fig. 13). The dimensions of elongated mitochondria showed insignificant changes when compared to control group (Fig. 3b). In addition, round mitochondria showed significant increase ( $p < 0.05$ ) in diameter compared to diabetic group (GB) (Fig. 3c). Dilated cross sections of rER cisterna were also observed in  $\alpha$  cell. Free ribosomes and numerous characteristic secretory granules were observed scattered in the cytoplasm (Fig. 13).

The  $\beta$  cells were also polygonal in shape with pleomorphic nuclei (Fig. 14a). In some cells slightly irregular and clefted nuclei were observed (Fig. 14b). In other cells the nuclei appeared round but with segregated nucleoli and indistinct nuclear envelope with dilated pores (Fig. 14c). Small sized nuclei were also observed in other cells (Fig. 14d). In most nuclei, an even distribution of chromatin was noted. However, reduced heterochromatin was observed in some nuclei (Fig. 14a). Numerous elongated mitochondria with dark matrices were observed scattered within the cytoplasm (Fig. 14b, d) although some round mitochondria were noted (Fig. 14d). The width of elongated



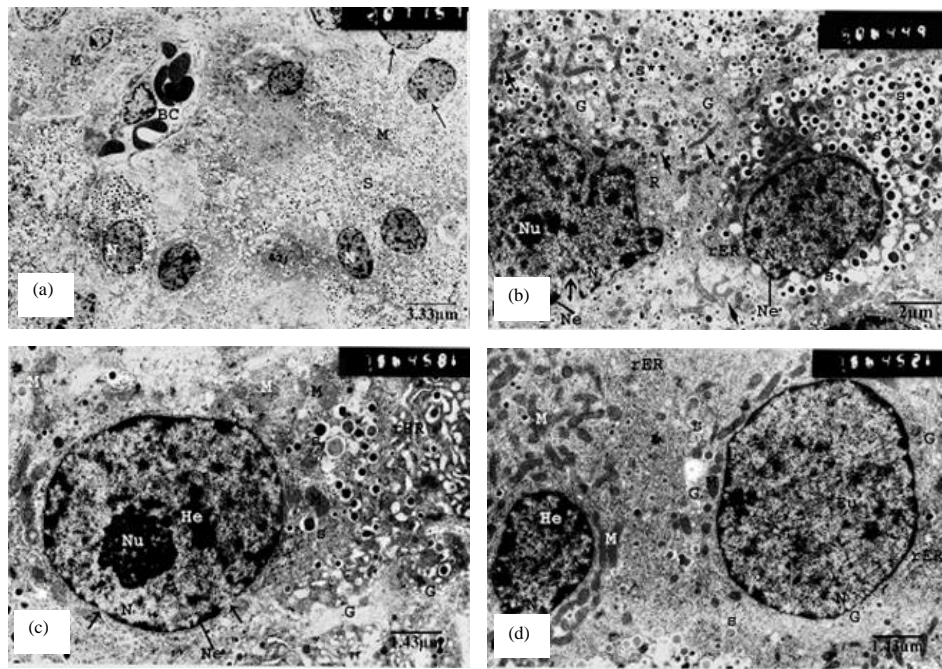


Fig. 14: E.M. Islets of Langerhans of diabetic rats-treated with thymoquinone (GE). (a) Illustrating, Islets of Langerhans of polygonal  $\beta$  cells scattered around a blood capillary (BC). Demonstrating;  $\beta$  cells with pleomorphic nuclei, reduced heterochromatin in some nuclei (arrow), and characteristic  $\beta$  secretory granules (s) in the apical portion. (b) Illustrating; irregular outline nucleus (N) with indistinct membranes of the nuclear envelope (Ne), a clefted nucleus (large arrow) with a prominent nucleolus (Nu) and indistinct nuclear envelope (Ne), small sized round and elongated mitochondria (M) with black arrow pointing at the elongated mitochondria displaying signs of fragmentation, small areas of Golgi cisterna (G), free ribosomes, polysomes, and the small sized characteristic  $\beta$  secretory granules (s). (c) Illustrating; a large sized round  $\beta$  cell nucleus (N), with a segregated nucleolus (Nu), indistinct nuclear envelope (Ne), few dilated nuclear pores (arrows), elongated (black arrow) and round mitochondria (M), the area of Golgi apparatus (G), the dilated rER cisterna and the  $\beta$  secretory granules (s). (d) Illustrating;  $\beta$  cell nuclei (N) of different sizes, with normal chromatin distribution, and indistinct nuclear envelope (Ne), elongated mitochondria (arrows), dilated Golgi cisterna (G), free ribosomes (R), and few small sized  $\beta$  secretory granules (s)

mitochondria showed significant decrease ( $p < 0.05$ ) compared to the control. In addition, both the length and width of elongated mitochondria showed significant increase ( $p < 0.05$ ) compared to diabetic group (Fig. 4b). Golgi cisterna (Fig. 14b) appeared dilated in some sections (Fig. 14d). The rER appeared as parallel stacked membrane bound cisterna or as cross sections both of which were dilated (Fig. 14b, c). Detached ribosomes were also observed within the cytoplasm. Numerous secretory granules of different sizes were observed scattered in the cytoplasm of  $\beta$  cells (Fig. 14b). A significant increase ( $p < 0.05$ ) in the diameter of large secretory granules compared to diabetic

(GB) and a significant decrease ( $p < 0.05$ ) compared to control (Fig. 4d) was noted. The small granules also demonstrated a significant increase ( $p < 0.05$ ) in diameter compared to diabetic group (GB) (Fig. 4e).

## DISCUSSION

The specific toxicity of STZ on pancreatic  $\beta$  cells has been studied in several experimental models (Aughsteen, 2000; Bolkent *et al.*, 2000; Mythili *et al.*, 2004). In addition various plants have been investigated for their antidiabetic effect and have shown ability to prevent degenerative and metabolic effects in STZ induced diabetic animal models (Yazdanparast *et al.*, 2005; Soleimani *et al.*, 2007; Bhandari *et al.*, 2007; Noor *et al.*, 2008). *Nigella sativa* has been used as antidiabetic in traditional medicine with many studies showing that *N. sativa* treatment can decrease blood glucose level in STZ induced diabetes (El-Dakhakhny *et al.*, 2002; Kanter *et al.*, 2003, 2004). However, there were no morphological studies examining the pancreas ultrastructure in rats treated with *N. sativa* extracts and thymoquinone.

In the present investigation no pathological changes were detected in the islets of control rats. In contrast, in STZ diabetic rats, light and electron micrographs revealed many changes in pancreatic islets. Relatively small and atrophied islets were noted. Inflammation in islets, extensive fibrosis in the connective tissue surrounding the blood vessels, vacuolation of the cytoplasm and degranulation were observed. These findings are consistent with the results of several studies which detected similar histological findings (Aughsteen, 2000; Kanter *et al.*, 2003, 2004; Mythili *et al.*, 2004; Yazdanparast *et al.*, 2005; Bhandari *et al.*, 2007; Soleimani *et al.*, 2007; Noor *et al.*, 2008; Azza Attia, 2009).

In STZ diabetic rats, electron microscope showed that  $\alpha$  cell secretory vesicles and organelles showed intact morphology without significant alterations. However, the mitochondria demonstrated significant decrease in dimension compared to the control group and displayed signs of fragmentation. In addition vacuolation of the cytoplasm was noted in some cells. Similar results were obtained by Mythili *et al.* (2004), where  $\alpha$  cells showed swelling of the mitochondria as well as cytoplasmic degranulation when treated with  $50 \text{ mg kg}^{-1}$  STZ. On the other hand,  $\beta$  cells showed several pathological changes.

The nuclei showed chromatin aggregation and reduced heterochromatin indicating DNA damage as well as increased number of dilated nuclear pores. It was suggested that these could be due to shrinkage of the nuclear material as a result of accumulation of secretory granules in acinar cells that pushed these nuclei to the periphery as mentioned by Azza Attia (2009). In addition some cells possessed irregular outline nuclei and some nuclei possessed inclusions.

The mitochondria appeared electron dense with some appearing vacuolated and others displaying signs of fragmentation. These changes can be interpreted as consequences of long term metabolic impairment. Degranulation was noted in several cells. In addition a diminishment in the granule contents as well as the number of secretory granule was detected which is most probably due to the decreased insulin synthesis. This is in agreement with the suggestion of Cotran *et al.* (1994) who stated that  $\beta$  cell degranulation is encountered in insulin dependent diabetes due to depletion of insulin stores. Both the mitochondria and the secretory granules showed a significant decrease in dimension compared to the control group. Dilation of Golgi and rER cisterna was observed. Cytoplasmic vesiculation and autophagic vacuoles were also noted. Autophagic vacuoles reflect the increased cellular damage and are a form of cellular reaction to tissue injury and physiologic stimuli (Hurban *et al.*, 1965). Similar pathological findings were detected in the studies

conducted by Aughsteen (2000), Bolkent *et al.* (2000) Mythili *et al.* (2004), Degirmenci *et al.* (2005) and Azza Attia (2009) on streptozotocin induced diabetic rats and mice.

Administration of *N. sativa* aqueous extract decreased some observations noted in the diabetic group. The islets appeared small in size and with reduced number of cells but of normal shape and architecture. The  $\alpha$  cells showed normal morphology. However, the mitochondria appeared with dark matrices and displayed normal distribution. In addition, most of the mitochondria displayed signs of fragmentation. The  $\beta$  cells of this group showed normal chromatin distribution with terminalized nucleoli in most nuclei although some nuclei demonstrated segregated nucleoli. The mitochondria displayed significant decrease in dimension compared to the control group but showed no signs of fragmentation. However, few mitochondria appeared vacuolated. In addition, the secretory granules showed dense core and a significant increase in diameter compared to the diabetic group. Very few granules appeared less dense or empty. No cytoplasmic vacuolation was noted.

Treatment of diabetic rats with the oil of *N. sativa* did not elaborate the destructive effect of STZ on islet cells. The islets appeared relatively small and irregularly shaped compared to control although there was an increase in number of islet cells compared to the diabetic group. In  $\alpha$  cells, many nuclei appeared euchromatic and the secretory granules showed significant reduction in size. The cytoplasm appeared disrupted displaying vacuoles and wide intercellular spaces were observed. On the other hand, administration of *N. sativa* oil aggravated the damaging effect of STZ on  $\beta$  cells. Nuclei showed significant decrease in their width compared to the other groups. The cells appeared degranulated although the size of the secretory granules was increased significantly but most of the granules were empty or possessed less dense cores. Very Few mitochondria were observed. It is important to note that the both round and elongated mitochondria showed significant increase in dimensions compared to the diabetic group. In addition, these dimensions were also increased compared to the control group but insignificantly, although their number was decreased. This may be explained as possible fusion of small sized mitochondria taking place. Disruption of the cytoplasm was also evident.

The use of thymoquinone; the active ingredient of *N. sativa*, ameliorated the toxic effects of STZ on pancreatic cells. The islets appeared with similar size to that detected in control thus displaying an increase in size as well as number of polygonal cells in comparison to diabetic group. However infiltration was noted in few islets in addition to infiltration of acinar cells. The electron micrographs showed that  $\beta$  cells retained their structures. However; some nuclei appeared heterochromatic and with small size and with dilated perinuclear space. The  $\beta$  cells retained their normal structure with its  $\beta$  granules. Few nuclei however appeared euchromatic. An increased number of mitochondria were noted in cytoplasm of  $\beta$  cells. They were significantly increased compared to diabetic group but were of smaller size compared to the control group. Lowell and Schulman (2005) stated that the increased number of mitochondria may reflect compensatory adaptation to produce much energy in response to glucose stimuli to maintain glucose homeostasis. The increased number of mitochondria can therefore be explained by their potency to adapt to metabolic changes by replicating to supply the energy for the synthesis and secretion of insulin. In contrast, vacuolated mitochondria with disrupted cristae noted in diabetic group reflect a limited capacity of mitochondria to overcome the oxidative stress in  $\beta$  cells.

In agreement with our findings, Kanter *et al.* (2003, 2004) showed that the use of *N. sativa* volatile oil reduced the severity of degenerative and necrotic changes in islets of STZ-diabetic rats. In that study sections of pancreatic tissues of treated rats stained with haematoxylin and eosin

showed that the majority of cells showed light degeneration compared to the diabetic group with no treatment. The islets were increased in size but there was lymphoid cell infiltration in peripheral parts of the islets (Kanter *et al.*, 2003, 2004). Similar findings were obtained using different plant extracts for treatment of STZ induced diabetes (Yazdanparast *et al.*, 2005; Soleimani *et al.*, 2007; Noor *et al.*, 2008). Yazdanparast *et al.* (2005) showed that *Teucrium polium* crude extract seems to be capable of regenerating the islets of Langerhans and enhancing insulin secretion. The methanolic extract of *Equisetium arvense* showed islet regeneration in STZ diabetic rats (Soleimani *et al.*, 2007). In addition aloe vera has shown similar effects (Noor *et al.*, 2008).

This is the only study to investigate the effect of *N. sativa* seed decoction, oil and thymoquinone on the cellular damage in pancreatic cells in STZ induced diabetic rats using the TEM. However, studies on other plants have shown similar findings (Azza Attia, 2009; Bolkent *et al.*, 2000; Arulselvan and Subramanian, 2007; Degirmenci *et al.*, 2005). Treatment of STZ diabetic rats with chard extract showed an increase in the number of  $\beta$  cells of Langerhans islets and in the secretory granules, together with many hypertrophic Golgi apparatus and granules of low densities. Degirmenci *et al.* (2005) demonstrated that acarbose and *Rumex patientia* L. protected the STZ induced morphological damage in  $\beta$  cells. Arulselvan and Subramanian (2007), suggested that *Murraya koenigii* leaves extract treatment exerts a protective effect in diabetes by decreasing oxidative stress and pancreatic  $\beta$  cell damage due to its antioxidant properties. Similarly, Azza Attia (2009) showed that administration of 3 mg of  $\beta$ -carotene three times/week to STZ diabetic rats protected pancreatic  $\beta$  cells from the damaging effect of STZ and that this effect is possibly mediated by the antioxidant effect of  $\beta$ -carotene.

In conclusion, our results emphasize that *N. sativa* extracts are effective in reducing the cellular damage caused by STZ. In addition, our findings suggest that the active ingredient thymoquinone is the most effective against STZ diabetes as its administration ameliorated most of the toxic effects. These effects could be attributed to the antioxidant properties of *N. sativa* and thymoquinone that prevent the cellular damage caused by STZ to the pancreatic tissue.

## REFERENCES

- ADA, 2008. Diagnosis and classification of diabetes mellitus. *Diabetes Care*, 31: S55-S60.
- Al-Enazi, M.M., 2007. Effect of thymoquinone on malformations and oxidative stress-induced diabetic mice. *Pak. J. Biol. Sci.*, 10: 3115-3119.
- Al-Hader, A., M. Aqel and Z. Hasan, 1993. Hypoglycemic effects of the volatile oil of *Nigella sativa* seeds. *Int. J. Pharmacol.*, 31: 96-100.
- Arulselvan, P. and S.P. Subramanian, 2007. Beneficial effects of *Murraya koenigii* leaves on antioxidant defense system and ultrastructural changes of pancreatic  $\beta$ -cells in experimental diabetes in rats. *Chem. Biol. Interactions*, 165: 155-164.
- Aughsteeen, A.A., 2000. An ultrastructural study on the effect of STZ on the islet of Langerhans in mice. *Electric Microscope*, 49: 681-690.
- Azza Attia, A., 2009. Histological and electron microscopic studies of the effect of  $\beta$ -Carotene on the pancreas of streptozotocin (STZ)-induced diabetic rats. *Pak. J. Biol. Sci.*, 12: 301-314.
- Bhandari, U., N. Jain and K.K. Pillal, 2007. Further studies on antioxidant potential and protection of pancreatic  $\beta$ -cells by *Embelia ribes* in experimental diabetes. *Exp. Diabetes Res.*, 2007: 15803-15809.
- Bolkent, S., R. Yanardag, O.A. Tabakoglu and S.O. Ozsoy, 2000. Effects of chard (*Beta vulgaris* L. var. cicla) extract on pancreatic B cells in streptozotocin-diabetic rats: A morphological and biochemical study. *J. Ethnopharmacol.*, 73: 251-259.

- Brownlee, M., 2005. The pathology of diabetic complications: A unifying mechanism. *Diabetes*, 54: 1615-1625.
- Burits, M. and F. Bucar, 2000. Antioxidant activity of *Nigella sativa* essential oil. *Phytother. Res.*, 14: 323-328.
- Cotran, R.S., V. Kumar and S.L. Robbins, 1994. Robbins Pathologic Basis of Disease. 5th Edn., WB Saunders Co., Philadelphia, London, Toronto, Montreal, Sydney, pp: 543-551.
- Degirmenci, I., M.C. Ustuner, Y. Kalender, S. Kalender and H.V. Gunes, 2005. The effects of acarbose and *Rumex patientia* L. on ultrastructural and biochemical changes of pancreatic  $\beta$  cells in streptozotocin-induced diabetic rats. *J. Ethnopharmacol.*, 97: 555-559.
- El-Alfy, T.S., H.M. El-Fatratry and M.A. Toama, 1975. Isolation and structure assignment of an antimicrobial principle from the volatile oil of *Nigella sativa* L. seeds. *Pharmazie*, 30: 109-111.
- El-Dakhakhny, M., N. Mady, N. Lember and H.P.T. Ammon, 2002. The hypoglycaemic effect of *Nigella sativa* oil is mediated by extrapancreatic actions. *Planta Medica*, 68: 463-464.
- El-Kamali, H.H., A.H. Ahmed, A.S. Mohammed, A.M.M. Yahia, I.H. El-Tayeb and A.A. Ali, 1998. Antibacterial properties of essential oils from *Nigella sativa* seeds, *Cymbopogon citratus* leaves and *Pulicaria undulata* aerial parts. *Fitoterapia*, 69: 77-78.
- El-Tahir, K.E., M.M. Ashour and M.M. Al-Harbi, 1993a. The respiratory effects of the volatile oil of the black seed (*Nigella sativa*) in guinea pigs: Elucidation of the mechanism(s) of action. *General Pharmacol.*, 24: 1115-1122.
- El-Tahir, K.E.H., M.M.S. Ashour and M.M. Al-Harbi, 1993b. The cardiovascular actions of the volatile oil of the black seed in rats. Elucidation of the mechanism(s). *General Pharmacol.*, 24: 1123-1131.
- Farida, M., F.M. Al-Awadi and K.A. Gumaa, 1987. Studies on the activity of individual plants of an antidiabetic plant mixture. *Acta Diabetol.*, 24: 37-41.
- Ganda, O.P., A.A. Rassini, A.A. Like and C. Boston, 1976. Studies on streptozotocin diabetes. *Diabetes*, 25: 595-595.
- Goreja, W.G., 2003. Black Seed: Natures Miracle Remedy. Amazon Herbs Press, New York, pp: 54.
- Hossain, P., B. Kavar and M. El-Nahas, 2007. Obesity and diabetes in the developing world-A growing challenge. *New Engl. J. Med.*, 356: 213-215.
- Houcher, Z., K. Boudiaf, M. Benboubetra and B. Houcher, 2007. Effects of methanolic extract and commercial oil of *Nigella sativa* L. on blood glucose and antioxidant capacity in alloxan-induced diabetic rats. *Pteridines*, 18: 8-18.
- Houghton, P.J., R. Zarka, B. de la Heras and J.R.S. Hoult, 1995. Fixed oil of *Nigella sativa* and derived thymoquinone inhibit eicosanoid generation in leukocytes and membrane lipid peroxidation. *Planta Med.*, 61: 33-36.
- Hurban, Z., H.D. Swift and D. Lewis, 1965. Effect of B-3-Furyllamine on the ultrastructure of the hepatocytes and pancreatic acinar cells. *Lab. Invest.*, 14: 70-80.
- Kanter, M., I. Meral, Z. Yener, H. Ozbek and H. Demir, 2003. Partial regeneration/proliferation of the  $\beta$ -cells in the islets of Langerhans by *Nigella sativa* L. in streptozotocin-induced diabetic rats. *Tohoku J. Exp. Med.*, 201: 213-219.
- Kanter, M., O. Coskun, A. Korkmaz and S. Oter, 2004. Effects of *Nigella sativa* on oxidative stress and  $\beta$ -cell damage in streptozotocin-induced diabetic rats. *Anat. Rec. A. Discov. Mol. Cell. Evol. Biol.*, 279: 685-691.
- Lowell, B.B. and G.I. Schulman, 2005. Mitochondrial dysfunction in type 2 diabetes. *Science*, 308: 389-394.

- Marles, R.J. and N.R. Fransworth, 1994. Plants as source of antidiabetic agents. *Econ. Med. Plant Res.*, 6: 149-187.
- Mythili, M.D., R. Vyas, G. Akila and S. Gunasekaran, 2004. Effect of streptozotocin on the ultrastructure of rat pancreatic islets. *Microscopy Res. Tech.*, 63: 274-281.
- Noor, A., S. Gunasekaran, A.S. Manickam and M.A. Vijayalakshmi, 2008. Antidiabetic activity of *Aloe vera* and histology of organs in streptozotocin-induced diabetic rats. *Curr. Sci.*, 94: 1070-1076.
- Reynolds, E.S., 1963. The use of lead citrate at high pH as an electron opaque stain in electron microscopy. *J. Cell Biol.*, 17: 208-212.
- Schleicher, P. and M. Saleh, 1998. *Black Seed Cumin: The Magical Egyptian Herb for Allergies, Asthma and Immune Disorders*. Healing Arts Press, Rochester, Vermont.
- Soleimani, S., F.F. Azarbaizani and V. Nejati, 2007. The effect of *Equisetum arvense* L. (Equisetaceae) in histological changes of pancreatic  $\beta$ -cells in streptozotocin-induced diabetic in rats. *Pak. J. Biol. Sci.*, 10: 4236-4240.
- Szkudelski, T., 2001. The mechanism of alloxan and streptozotocin action in B cells of the rat pancreas. *Physiol. Res.*, 50: 537-546.
- Worthen, D., O. Ghoshen and P. Crooks, 1998. The *in vitro* anti-tumor activity of some crude and purified components of black seed, *Nigella sativa*. *Anticancer Res.*, 18: 1527-1533.
- Yazdanparast, R., M.A. Esmaeili and J.A. Helan, 2005. Teucrium polium extract effects pancreatic function of streptozotocin diabetic rats: A histopathological examination. *Iran Biomed. J.*, 6: 81-85.